Nuclear Physics B269 (1986) 170–204
North-Holland, Amsterdam

CORRELATIONS AND STATIC ENERGIES IN THE STANDARD HIGGS MODEL

I. MONTVAY

Deutsches Elektronen-Synchrotron DESY, Hamburg, F.R. Germany

Received 24 January 1985
(Revised 18 November 1985)

Correlations in the W-boson and Higgs boson channels and the static energy of an external SU(2) doublet charge pair are investigated by Monte Carlo calculations in the SU(2) lattice gauge theory with a scalar Higgs doublet field. The mass ratio m_W/m_H and the shape of the static potential are used to obtain information on the renormalization group trajectories in the three-dimensional coupling constant space. As a function of an appropriately chosen variable, the measured quantities are, within errors, independent from the scalar self-coupling (λ) in a wide range $0.1 \leqslant \lambda \leqslant \infty$. In the Higgs phase, a lower bound $m_H/m_W \geqslant (1.0 \pm 0.3)$ is obtained for the ratio of the Higgs boson mass to the W-boson mass.

1. Introduction

In the standard SU(3) ⊗ SU(2) ⊗ U(1) model the two non-abelian gauge symmetry factors play rather different rôles. The local gauge symmetry corresponding to SU(3)-colour is unbroken, the SU(3)-colour charges are confined and the colour interaction is strong. The local SU(2) gauge symmetry, on the other hand, is broken by the expectation value of the Higgs-doublet field, the SU(2) charges are screened and the corresponding interaction is weak. Since the values of the coupling constants are changing ("running" or "sliding") according to the renormalization group, the meaning of strong and weak coupling has to be explained in more detail. (For a review and an extensive list of references on the renormalization group see [1].) The renormalization group invariant meaning of "strong interaction" is that the SU(3)-colour coupling is of order 1 at the scale of hadron masses:

$$\alpha_{SU(3)}(M_{\text{hadron}}) = o(1). \tag{1.1}$$

In contrast to eq. (1.1), for the SU(2) coupling at the W-boson mass (m_W) experiments imply

$$\alpha_{SU(2)}(m_W) \simeq 0.04. \tag{1.2}$$

In principle, the non-abelian SU(2) interaction, too, can become strong at some very low energy scale, but this has no practical consequences because of the short range of the interaction due to the massive SU(2) gauge boson exchange. The theoretical consequence of eq. (1.2) is that the SU(2) ⊗ U(1) electroweak interaction can be treated by perturbation theory. The impressive success of the perturbative approach culminated not very long ago in the discovery of W- and Z-bosons at precisely the predicted mass [2].

The only remaining source of uneasiness in the standard model is buried in the Higgs sector incorporating the inherently non-perturbative phenomenon of spontaneous symmetry breaking. The main interest of the non-perturbative investigation of the electroweak theory lies, in fact, in the deeper understanding of the Higgs mechanism [3], which renders the W- and Z-bosons, the leptons and quarks and the, up to now elusive, Higgs boson a mass.

STRONG WEAK-INTERACTIONS

In the present paper the Higgs sector of the standard SU(2) ⊗ U(1) electroweak theory is investigated by the non-perturbative numerical Monte Carlo method (for references and a collection of papers see [4]). The calculation is performed in a coupling constant range, where eq. (1.2) is not fulfilled. On the contrary, similarly to eq. (1.1), we shall typically consider the case

$$\alpha_{SU(2)} \simeq o(1) \tag{1.3}$$

i.e. the values of the coupling constants will correspond to a situation where the SU(2) weak interaction is strong. The electromagnetic interaction will be neglected altogether (no U(1)-factor) and no fermions (leptons and quarks) will be considered. For a possibility of how to include these in the lattice action, see ref. [5].

The study of the standard SU(2) Higgs sector in the situation corresponding to eq. (1.3) is interesting from several points of view:

(i) It can reveal the existence of non-perturbative constraints in the electroweak theory. For instance, the number of independent renormalized couplings can be smaller than the number of bare couplings. A large body of evidence [6] has been collected to support the occurence of such a "parameter reduction" in the single-component ϕ^4 theory, where the renormalized coupling is probably always zero.

(ii) It is interesting to compare and confront the behaviour of the totally broken SU(2) gauge interaction with unbroken SU(N) colour, studied up to now in most Monte Carlo investigations.

(iii) The gauge-Higgs system is theoretically interesting for its own sake, as a representative of a class of quantum field theories.

(iv) Finally, there has been some speculations that weak interactions could become strong in the hundred GeV energy range [7]. This possibility seems to be improbable at present, but direct experimental evidence is still scarce at such high energies.

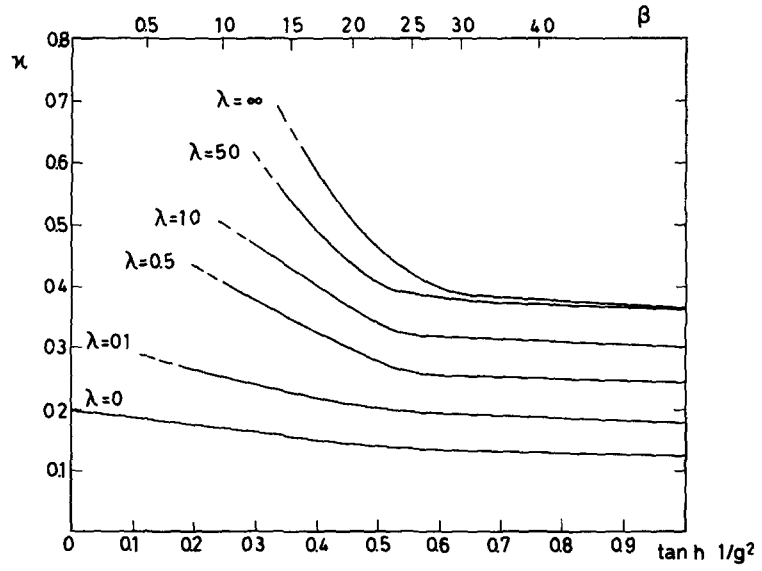

Fig. 1. The phase transition lines in the (g^{-2}, κ) plane for constant λ according to fig. 3 in ref. [9].

Previous Monte Carlo simulations of the SU(2)-Higgs system with scalar field in the fundamental representation [8–11] concentrated mainly on the singularity structure in the coupling constant space. These studies showed that there is a phase transition surface separating the Higgs phase from the confining phase. These "phases" are, however, not qualitatively different from each other [12], they are continuously connected beyond the edge of the critical surface. This structure is illustrated by fig. 1, which is a reproduction of fig. 3 of the paper by Kühnelt, Lang and Vones [9].

An interesting question is the order of the phase transition separating the Higgs-like and confinement-like regions. If there is a critical surface corresponding to a second-order phase transition, then the correlation length becomes infinite and some continuum theory can be defined in a limit going to this surface. (The continuum theory may be trivial, i.e. noninteracting, except perhaps for some peculiar "fixed points" on this surface.) Information on the critical behaviour can be obtained, e.g. from "finite size scaling" [10] or from a direct study of the correlations [11].

In my previous paper [11] the correlations were numerically calculated in the limit of infinite self-coupling ($\lambda \to \infty$; fixed-length Higgs field on the lattice). This limit of the standard electroweak theory was considered extensively in the literature [13] as an interesting limiting case, when the tree-level mass of the physical Higgs boson tends to infinity. (The physical mass can, however, stay finite [14].) The results in ref. [11] showed, that in the vicinity of the phase transition line the correlation lengths in

both the isovector 1^{--} (W-boson) and isoscalar 0^{++} (Higgs boson) channels have a tendency to grow. This can be interpreted as a sign for a second-order phase transition, but a weakly first-order transition with some small specific heat is equally possible. The present paper is an extension of ref. [11]: in the case of the fixed-length Higgs field ($\lambda = \infty$) more statistics are collected closer to the critical line and the variable-length case is considered, too, for several values of the self-coupling λ. The precise position of the phase transition is determined at several points directly from the correlations. Another important limit, namely $\beta = \infty$ (no gauge coupling) [15] is also considered. Special emphasis is given to the information which can be obtained from the mass ratios and from the static potential concerning the renormalization group properties of the model.

In the next section, after summarizing the lattice formulation of the SU(2) fundamental Higgs model, the results for the correlations will be presented and discussed. In sect. 3 the static energy of an external SU(2) doublet charge pair is considered and consequences for the renormalization group trajectories ("lines of constant physics") in the three-dimensional coupling constant space will be discussed. The last section contains the conclusions.

2. Correlations

2.1. THE LATTICE ACTION

The continuum euclidean action S_c of an SU(2) gauge field interacting with a complex scalar doublet $\phi(x)$ can be written like

$$S_c = \int d^4x \left\{ \tfrac{1}{2} \mathrm{Tr}\big(F(x)_{\mu\nu} F(x)_{\mu\nu}\big) + D_\mu \phi^\dagger(x) D_\mu \phi(x) + \lambda_c \big(\phi^\dagger(x)\phi(x) - v^2\big)^2 \right\}. \tag{2.1}$$

Here $F(x)_{\mu\nu}$ denotes, as usual, the field-strength matrix of the gauge field, D_μ is the gauge-covariant derivative, λ_c is the self-coupling of the Higgs field and v is the tree-level vacuum expectation value related to the opposite-sign mass term $-\mu^2 \phi^\dagger(x)\phi(x)$ by

$$v = \frac{\mu\sqrt{2}}{\sqrt{\lambda_c}}. \tag{2.2}$$

The gauge field is described on the lattice by the link variables $U(x, \mu) \in \mathrm{SU}(2)$ and the Wilson gauge lattice action is a sum Σ_P over positive orientation plaquettes P. For the lattice description of the Higgs field it is convenient to introduce the lattice

site variable ϕ_x and the lattice bare couplings κ, λ by the replacements

$$a\phi(ax) \to \sqrt{\kappa}\,\phi_x\,,$$

$$\lambda_c \to \lambda\kappa^{-2}\,,$$

$$8-(a\mu)^2 \to (1-2\lambda)/\kappa\,. \tag{2.3}$$

Here a denotes, as usual, the lattice spacing. In these variables the euclidean lattice action is

$$S=\sum_x\left\{\lambda\left(\phi_x^\dagger\phi_x-1\right)^2+\phi_x^\dagger\phi_x-\kappa\sum_\mu\phi_{x+\mu}^\dagger U(x,\mu)\phi_x\right\}+\beta\sum_{\mathrm{P}}\left\{1-\tfrac{1}{2}\,\mathrm{Tr}\,U_{\mathrm{P}}\right\}. \tag{2.4}$$

The lattice is assumed to be periodic in all four directions. Σ_x means a summation over all lattice sites, Σ_μ is a sum over positive and negative directions ($\mu=\pm1,\pm2,\pm3,\pm4$), $x+\mu$ is the neighbouring point of x in the direction μ and β is related to the bare gauge coupling g by $\beta=4/g^2$.

The peculiarity of the SU(2) doublet field ϕ_x is that it can also be represented by its length $\rho_x\geqslant 0$ and by an SU(2) matrix α_x. The correspondence is given by ($\alpha=1,2$):

$$\phi_x^\alpha=\rho_x\alpha_{x,\alpha 2}\,,$$

$$\tilde{\phi}_x^\alpha=\varepsilon_{\alpha\beta}\phi_\beta^\dagger=\rho_x\alpha_{x,\alpha 1}\,. \tag{2.5}$$

Here $\tilde{\phi}$ is the opposite hypercharge doublet field in SU(2) $\otimes$ U(1) (ε is the antisymmetric unit tensor). Using the new variables, the lattice action can be written as

$$S=\beta\sum_{\mathrm{P}}\left(1-\tfrac{1}{2}\,\mathrm{Tr}\,U_{\mathrm{P}}\right)+\sum_x\Big\{\rho_x^2-3\log\rho_x+\lambda\left(\rho_x^2-1\right)^2$$

$$-\kappa\sum_{\mu>0}\rho_{x+\mu}\rho_x\,\mathrm{Tr}\left(\alpha_{x+\mu}^\dagger U(x,\mu)\alpha_x\right)\Big\}. \tag{2.6}$$

The integration measure was originally $\rho_x^3\,\mathrm{d}\rho_x\,\mathrm{d}^3\alpha_x\,\mathrm{d}^3U(x,\mu)$ (if d^3g denotes the invariant Haar-measure in SU(2)), but in eq. (2.6) the factor ρ_x^3 is included in the exponent, therefore the measure is simply $\mathrm{d}\rho_x\,\mathrm{d}^3\alpha_x\,\mathrm{d}^3U(x,\mu)$. Let us introduce, instead of the SU(2) link- and site-variables $U(x,\mu)$ and α_x, the gauge invariant link variable

$$V(x,\mu)\equiv\alpha_{x+\mu}^\dagger U(x,\mu)\alpha_x\,. \tag{2.7}$$

Due to local gauge invariance, this can be used for the description of the gauge field

also in the pure gauge part, therefore the lattice action can be written as

$$S = \beta \sum_{\mathrm{P}} \left(1 - \tfrac{1}{2} \operatorname{Tr} V_{\mathrm{P}}\right) + \sum_{x} \left\{ \rho_x^2 - 3 \log \rho_x + \lambda \left(\rho_x^2 - 1\right)^2 - \kappa \sum_{\mu > 0} \rho_{x+\mu} \rho_x \operatorname{Tr} V(x, \mu) \right\}. \tag{2.8}$$

This does not depend on α_x, therefore the integration $\mathrm{d}^3\alpha_x$ gives only an inessential constant factor, and can be omitted. The integration measure for eq. (2.8) is $\mathrm{d}\rho_x \, \mathrm{d}^3 V(x, \mu)$. The disappearence of the angular part α_x of the Higgs field is usually expressed by saying that it is "eaten" by the gauge field. Since both ρ_x and $V(x, \mu)$ are gauge invariant, both of them describe physical degrees of freedom: $V(x, \mu)$ corresponds to the (gauge-) W-boson and ρ_x to the physical (Higgs) H-boson.

The SU(2) Higgs model with Higgs field in the fundamental representation has a global SU(2) "weak-isospin" symmetry. In the full SU(2) $\otimes$ U(1) electroweak theory this symmetry corresponds to the transformations $\ell \to \nu_\ell$ ($\ell = \mathrm{e}, \mu, \tau$), $\mathrm{u} \leftrightarrow \mathrm{d}$, $\mathrm{c} \leftrightarrow \mathrm{s}$, $\mathrm{t} \leftrightarrow \mathrm{b}$; therefore it is broken by electromagnetism and by fermion mass differences within doublets. In the action (2.8) the exact global weak-isospin symmetry transformation is

$$V'(x, \mu) = U^{-1} V(x, \mu) U,$$

$$\rho'_x = \rho_x. \tag{2.9}$$

For comparison, the local gauge transformation is

$$U'(x, \mu) = U_{x+\mu}^{-1} U(x, \mu) U_x,$$

$$\alpha'_x = U_x^{-1} \alpha_x,$$

$$\alpha_x^{\dagger\prime} = \alpha_x^{\dagger} U_x,$$

$$V'(x, \mu) = V(x, \mu). \tag{2.10}$$

With respect to weak isospin the W-boson is isovector, the Higgs boson is isoscalar.

There are interesting limits of the model, which can be studied separately. In the case of infinitely strong self-coupling $\lambda \to \infty$ the length of the Higgs field is frozen to $\rho_x = 1$, and the action is

$$S_{\lambda = \infty} = \beta \sum_{\mathrm{P}} \left(1 - \tfrac{1}{2} \operatorname{Tr} V_{\mathrm{P}}\right) - \kappa \sum_{x, \mu > 0} \operatorname{Tr} V(x, \mu). \tag{2.11}$$

The correlations in this limit were investigated in ref. [11]. This is the limit of a very strongly interacting Higgs field, where μ and λ_{c} in eq. (2.2) go to infinity in such a

way that the tree-level vacuum expectation value $v \simeq a^{-1}\sqrt{\kappa}$ remains constant. The tree-level mass $\mu\sqrt{2}$ of the physical Higgs boson goes also to infinity. Nevertheless, as it was shown in ref. [11] and as we shall see below in more detail, the lowest mass in the isoscalar 0^{++} channel remains finite.

Another important limit of the actions in eqs. (2.6), (2.8) is $\beta \to \infty$ (zero gauge coupling). In this case the link variable $U(x, \mu)$ is a pure gauge, therefore it is necessary to restore the angular Higgs variable α_x and return to eq. (2.6), which gives

$$S_{\beta=\infty} = \sum_x \left\{ \rho_x^2 - 3\log\rho_x + \lambda\left(\rho_x^2 - 1\right)^2 - \kappa \sum_{\mu>0} \rho_{x+\mu}\rho_x \mathrm{Tr}\left(\alpha_{x+\mu}^\dagger \alpha_x\right) \right\}. \quad (2.12)$$

This is the lattice version [15] of the Gell-Mann-Lévy linear σ-model [16]. It has a global SU(2) $\otimes$ SU(2) symmetry corresponding to the transformation ($U_\pm \in$ SU(2)):

$$\alpha'_x = U_-^{-1} \alpha_x U_+ . \quad (2.13)$$

SU(2) $\otimes$ SU(2) is equivalent to O(4) and the SU(2) group elements can also be represented by a unit-length four-vector (a_0, a_r):

$$a_x = a_{0,x} + i\tau_r a_{r,x} \qquad (\tau_r = \text{Pauli matrix}). \quad (2.14)$$

In the limit $\lambda \to \infty$ the model in eq. (2.12) becomes the non-linear σ-model in four dimensions:

$$S_{\beta=\infty,\lambda=\infty} = -2\kappa \sum_{x,\mu>0} a_{\rho,x+\mu} a_{\rho,x} . \quad (2.15)$$

In the continuum limit the action $S_{\beta=\infty}$ is expected to describe 3 massless Goldstone bosons and 1 massive scalar particle, which are presumably non-interacting [17].

2.2. MONTE CARLO CALCULATION OF THE CORRELATIONS

The Monte Carlo simulation in the SU(2) fundamental Higgs model can be done by using the lattice action in eq. (2.8). For the fixed-length case ($\lambda = \infty$) the corresponding action is (2.11). In order to see whether the use of gauge invariant variables makes some difference, I did parallel test runs with the actions in eqs. (2.6) and (2.8) at the points $\lambda = 1.0$; $\beta = 2.3$; $\kappa = 0.30$ and 0.31. No appreciable difference could be observed either in the results or in the time-correlations during the updating. Since these are typical parameter values for the present work, this means that the simpler gauge invariant action can be safely used in our range. For very large $\beta \gg 1$ values, however, the original action (2.6) is expected to be better for the Monte Carlo updating, because the "hidden" angular Higgs degrees of freedom are crucial. At $\beta = \infty$ the gauge degrees of freedom are absent, therefore one has to use the action (2.12).

In the present paper the correlations were computed on an 8^4 lattice. The SU(2) link variables were replaced in most cases by the elements of the 120-dimensional icosahedral subgroup. The updating was done by the Metropolis method with 6 hits

per link for the gauge field $V(x, \mu)$ and 6 hits per site for the length variable ρ_x. The links and sites were updated in a random order, but always full sweeps were performed alternating over links and sites.

Diagonal correlations (and sometimes a few off-diagonal ones) were measured in different channels. In all cases the three-momentum was projected out both to $\boldsymbol{p} = 0$ and $\boldsymbol{p} = \pi/4a$ (1 in lattice units) in all three space-like directions. The time slices were chosen in all four possible time orientations. The measurement of the correlations was performed only after every 5th or 10th full sweeps, in order to reach more independent configurations. The results given below were collected typically from 8000–10 000 sweeps per point in the coupling constant space. The configuration was started in most cases from a previously equilibrated one in some neighbouring point. At least 1000 equilibrating sweeps were performed before starting to collect data for the correlations. The computer time used for the calculation of the correlations amounted to about 400 CPU hours on the Siemens 7.882 at the University of Hamburg.

To obtain the correlation lengths in the W-boson channel an appropriate operator is

$$O_{\mathrm{W}r}^{(m)} = \mathrm{Tr}\left\{\tau_r V(x, m)\right\} \qquad (m, r = 1, 2, 3). \tag{2.16}$$

As it was discussed in ref. [11], this has weak-isospin $I_{\mathrm{W}} = 1$ and spin-parity $J^{PC} = 1^{--}$. For the $I_{\mathrm{W}} = 0$ Higgs boson channel there are several possibilities:

$$O_{\mathrm{G}} = \sum_{(m,n)} \mathrm{Tr}\, V_{\mathrm{P}(m,n)},$$

$$O_{\mathrm{H}} = \rho_x,$$

$$O_{\mathrm{A}} = \sum_{m} \mathrm{Tr}\, V(x, m). \tag{2.17}$$

The first is the symmetric combination of the three space-like orientation single plaquette operators, which is often used in QCD glueball spectrum calculations for the 0^{++} channel. The second is the genuine $I_{\mathrm{W}} = 0$, $J^{PC} = 0^{++}$ Higgs variable (the length of the Higgs field). The third operator appears in the $\lambda = \infty$ action (2.11). Assuming that the 0^{++} state is the lowest isoscalar state, the symmetrization in O_{G} and O_{A} can also be omitted, provided that the correlation is determined at large enough distances and therefore the higher mass contributions from other spin-parity channels can be neglected. Similarly, the lowest mass can also be inferred from off-diagonal correlations, like e.g. between $\mathrm{Tr}\, V(x, m)$ and $\mathrm{Tr}\, V(x, n)$ $(m \neq n)$, if the distance is large enough.

The results obtained for the correlations in the W- and H-boson channels are shown in figs. 2a–2c and in table 1. Always the inverse correlation lengths are given, i.e. the estimates of the lowest mass in lattice units in the given channel. Table 1 also contains some global average quantities like the average link L, average plaquette P,

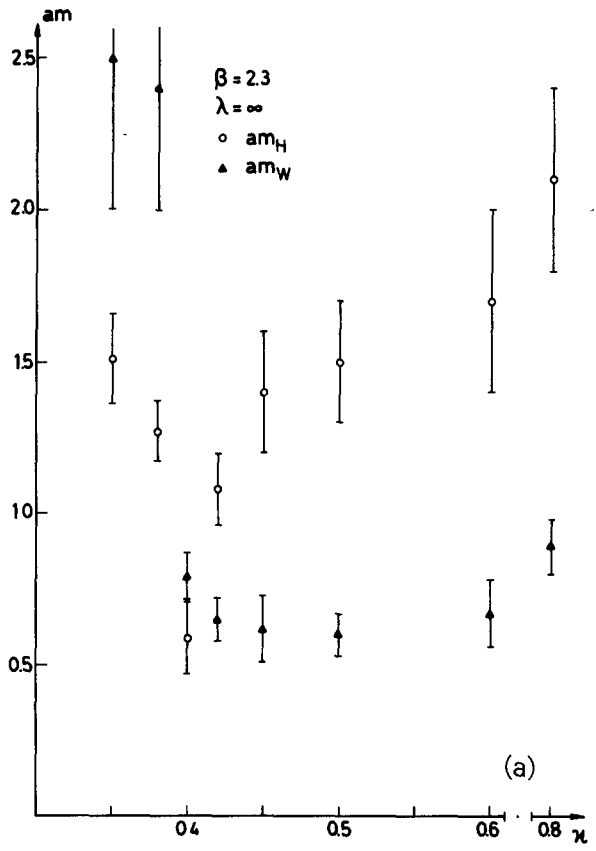

Fig. 2a. The inverse correlation lengths in the W-boson (am_W) and Higgs-boson (am_H) channel in lattice units for $\lambda = \infty$, $\beta = 2.3$.

average length ρ, length dispersion σ_ρ and average action per site s. These are defined, respectively, like

$$L = \left\langle \tfrac{1}{2} \operatorname{Tr} V(x,\mu) \right\rangle ,$$

$$P = \left\langle 1 - \tfrac{1}{2} \operatorname{Tr} V_P \right\rangle ,$$

$$\rho = \langle \rho_x \rangle ,$$

$$\sigma_\rho = \sqrt{\langle \rho_x^2 \rangle - \langle \rho_x \rangle^2} ,$$

$$s = 6\beta \left\langle 1 - \tfrac{1}{2} \operatorname{Tr} V_P \right\rangle + \left\langle \rho_x^2 - 3 \log \rho_x + \lambda \left(\rho_x^2 - 1 \right)^2 \right\rangle$$

$$+ 8\kappa \left\langle 1 - \tfrac{1}{2} \rho_x \rho_{x+\mu} \operatorname{Tr} V(x,\mu) \right\rangle . \qquad (2.18)$$

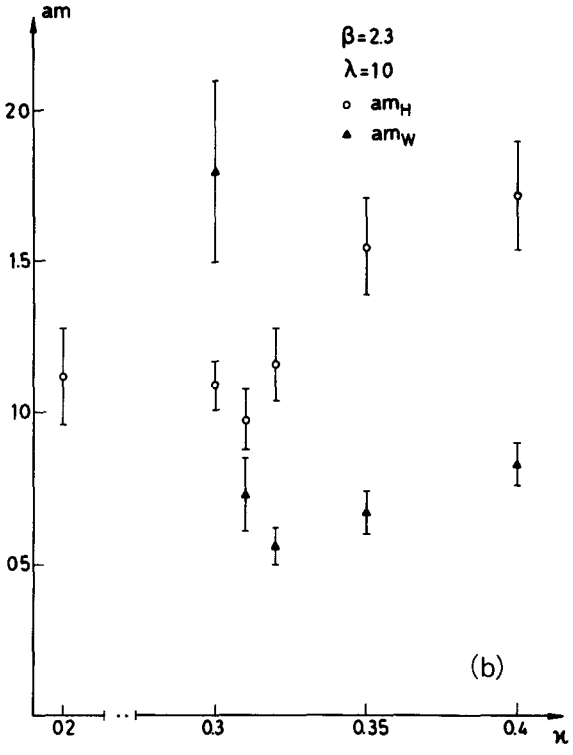

Fig. 2b. The same as fig. 2a, for $\lambda = 1.0$, $\beta = 2.3$

In the average action per site the constant term 8κ is added with respect to eq. (2.8), in analogy to the constant 6β in the average plaquette term. In the W-boson channel, for $am_W \leqslant 1$, the correlation can be determined, with relatively small error, up to the maximum distance $d = 4$ on the 8^4 lattice. The correlations in some sample points were shown in ref. [11]. The qualitative behaviour is here rather similar. The ease of measurement of correlations at larger distances recalls the general behaviour in 2-dimensional σ-models (see e.g. [18]) and not the pure SU(2) gauge theory, where it is rather difficult to obtain large-distance correlations (see e.g. [19]). For $am_W \geqslant 1.5$ the correlation drops fast at small distances. In such points the mass estimate is obtained from distance $d = 1$ (or at most from $d = 2$), therefore these points have larger systematic errors. The errors shown include some subjective estimate of the systematic errors, too.

In the case of the Higgs boson channel the situation is more involved. The one-plaquette operator O_G in eq. (2.17) behaves rather similarly, or even still somewhat worse, than in pure SU(2) gauge theory, i.e. the correlation usually cannot be determined beyond $d = 1$. The best points for O_G are below the phase transition line ($\kappa < \kappa_{cr}$, see below), where the behaviour, and also the value of the correlation

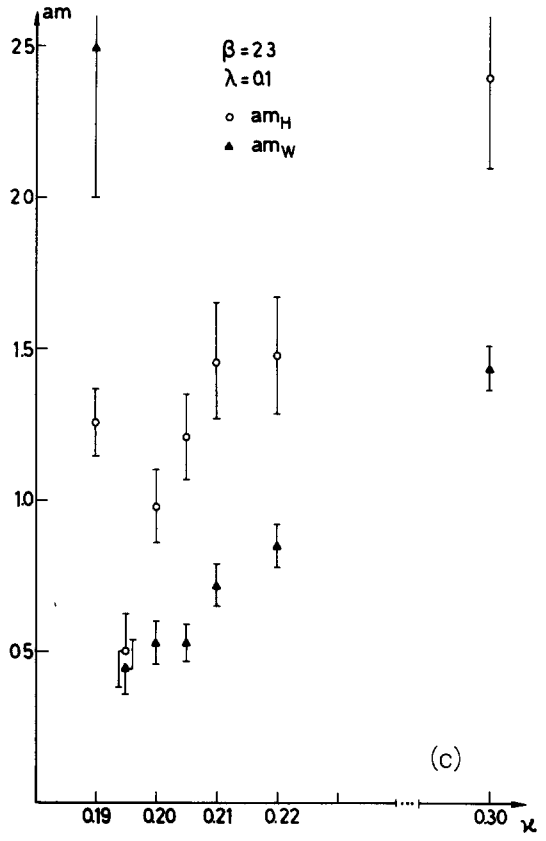

Fig 2c The same as fig. 2a, for $\lambda = 0.1$, $\beta = 2.3$.

length, is rather similar to pure SU(2) gauge theory at the same β-value [19]. The other two operators O_H and O_A behave oppositely: for $\kappa < \kappa_{cr}$ they are worse, for $\kappa > \kappa_{cr}$, however, much better than O_G. For $\kappa > \kappa_{cr}$ the diagonal correlation of O_H and O_A can be determined, within the given statistics, up to $d = 2$ or $d = 3$. O_A behaves for $\lambda > 0.1$ still somewhat better than O_H, but the mass estimates from O_A and O_H are always compatible. In the figures and in table 1 always the best estimate for am_H is given, sometimes also including information from the off-diagonal correlation between $\mathrm{Tr}\, V(x, m)$ and $\mathrm{Tr}\, V(x, n)$ $(m \neq n)$.

The energies E_1 obtained from the $\boldsymbol{p} = 1$ correlations give in most cases, within errors, the same masses $m = \sqrt{E_1^2 - \boldsymbol{p}^2}$ as the $\boldsymbol{p} = 0$ time slices. This shows that Lorentz invariance is approximately restored in the measured points. There seem to exist, however, some systematic deviations in the points with largest correlation lengths ($\xi \sim 2$), where the $\boldsymbol{p} = 1$ mass is usually 10–20% higher. This may be due to finite size effects, since finite cut-off effects are expected to become smaller for large ξ.

TABLE 1
The value of the W-boson mass (am_W) and Higgs-boson mass (am_H) in lattice units

λ	κ	am_W	am_H	L	P	s	ρ	σ_ρ
∞	0 35	2 5(5)	1 51(15)	0 2011(3)	0 3954(4)	8.693(5)		
∞	0 38	2 4(4)	1.27(9)	0 2318(4)	0 3931(6)	8.760(6)		
∞	0 4	0 79(8)	0 59(12)	0 2948(26)	0 3820(13)	8.528(15)		
∞	0 42	0.65(7)	1 08(12)	0 3437(11)	0.3757(3)	8.390(4)		
∞	0 45	0.62(11)	1 4(2)	0.3993(3)	0.3696(5)	8.263(6)		
∞	0 5*	0.60(7)	1 5(2)	0.4669(4)	0 3623(3)	8 132(4)		
∞	0 6*	0 67(11)	1.7(3)	0 5574(2)	0 3512(3)	7 971(3)		
∞	0 8*	0 89(9)	2.1(3)	0 6596(2)	0 3348(3)	7 799(4)		
1 0	0 2	4 0(5)	1 12(16)	0 1181(3)	0.3973(2)	8.300(6)	1 060	0.260
1 0	0 3	1.8(3)	1 09(8)	0.2316(2)	0.3924(2)	8 547(3)	1 115	0 258
1 0	0 31	0 73(12)	0 98(10)	0 3216(4)	0 3772(3)	8 080(7)	1 152	0 250(2)
1 0	0 32	0 56(6)	1 16(12)	0.3786(6)	0 3709(2)	7 821(9)	1.178	0 252(2)
1 0	0 35	0.67(7)	1.55(16)	0 4919(4)	0.3583(2)	7 256(6)	1.241	0.243
1.0	0 4	0 83(7)	1 72(18)	0 6101(5)	0 3425(2)	6 432(9)	1 331	0.228
0.5	0 25	2 7(5)	1.25(14)	0.1957(6)	0 3951(3)	8 318(6)	1 164	0 306
0 5	0.3	0 68(7)	1 34(18)	0 5009(3)	0 3569(2)	6 821(8)	1 358	0 292
0 1	0.19	2 5(5)	1.26(11)	0.2064(2)	0.3939(2)	7 775(11)	1 353	0 420
0 1	0 195	0 45(9)	0 50(12)	0 3159(3)	0.3771(2)	7 220(32)	1 450	0 429
0 1	0 2	0 53(7)	0 98(12)	0.4238(8)	0.3650(4)	6 673(15)	1 558	0.433
0 1	0 205	0 53(6)	1.21(14)	0 4879(5)	0 3577(2)	6 301(9)	1.636	0 432
0 1	0 21	0 72(7)	1 46(19)	0 5428(3)	0.3510	5 939(3)	1 712	0 427
0 1	0 22	0 85(7)	1 48(19)	0.6199(6)	0.3399(2)	5.298(10)	1 845	0 410
0 1	0 3	1 47(7)	2.4(3)	0.8415(2)	0 2728	0.187	2 628	0.327

The global average quantities L, P, ρ, σ_ρ and s are defined in eq (2 18). The errors in the last numerals are given in paranthesis If no error is given, the error estimate is $\leqslant 1$ in the last digit The β-value is always $\beta = 2\,3$. The lines with an asterisk were obtained with full SU(2) group, the rest with the icosahedral subgroup

2 3 BEHAVIOUR NEAR THE PHASE TRANSITION

The qualitative behaviour of am_W and am_H for $\beta = 2.3$, $\lambda = \infty$ (fig. 2a), $\beta = 2.3$, $\lambda = 1.0$ (fig. 2b) and $\beta = 2.3$, $\lambda = 0.1$ (fig. 2c) is quite similar. The main difference is in the widths of the κ-range, where similar changes occur: the region in the phase transition is squeezed for small λ. The reason for this behaviour is quite clear: at $\lambda = 0$ the model defined by the action (2.8) has a kinematical singularity. In the Higgs phase, where the link expectation value is substantial ($L \to 1$ for $\kappa \to \infty$), for large enough "hopping parameter" κ, the hopping term proportional to κ wins over the stabilizing ρ_x^2 term and the action is unbounded from below if $\rho_x \to \infty$. For very small λ the $\lambda(\rho_x^2 - 1)^2$ term can stabilize the theory only for very large ρ_x, therefore the change above κ_{cr} is squeezed into a small κ-region, which is asymptotically proportional to $\sqrt{\lambda}$.

Apart from the squeezing, there is a remarkable universal behaviour for different λ. This can already be seen in the global averages given in table 1. For instance, the

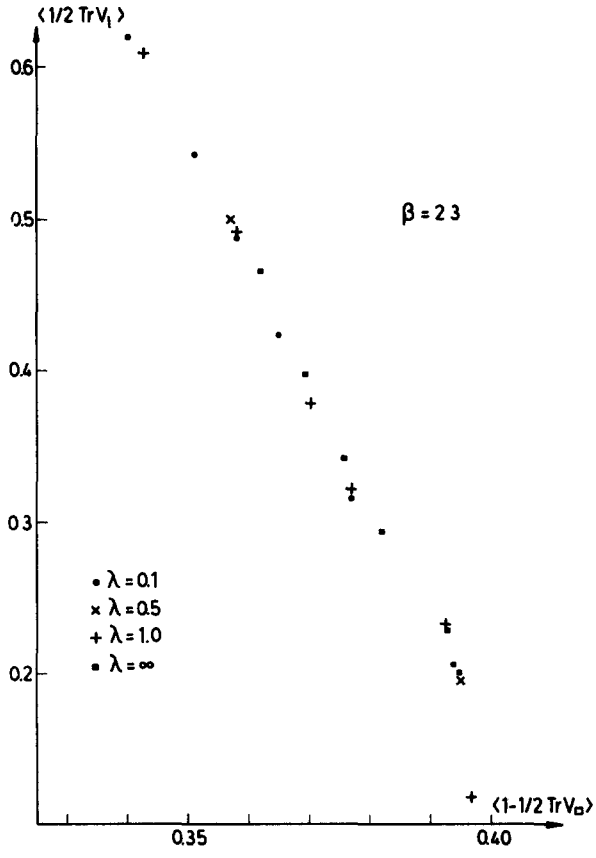

Fig. 3 The link expectation value $L = \langle \frac{1}{2} \mathrm{Tr}\, V_\ell \rangle$ as a function of the plaquette expectation value $P = \langle 1 - \frac{1}{2} \mathrm{Tr}\, V_\mathrm{P} \rangle$ for different λ-values at $\beta = 2.3$.

link expectation value is a universal function of the plaquette expectation value (see fig. 3). This shows, that κ is not the correct variable to use. Plotting the W-boson mass as a function of the link expectation value, one obtians the remarkable universal curve shown in fig. 4a. The same for the Higgs boson mass, in fig. 4b, shows a universal behaviour, too, although the errors are larger and maybe there is some mild tendency for the $\lambda = 0.1$ points to fall somewhat below the rest. Fig. 4b has to be contrasted, however, with the tree-level prediction $m_\mathrm{H} = v\sqrt{\lambda_\mathrm{c}}$, according to which m_H should go to infinity for $\lambda \to \infty$.

The approximate universality of the physical quantities in such a considerable λ-range may appear rather surprising at first sight. (Besides the masses, the static energy of an external SU(2) charge pair, considered in the next section, shows the same universality too.) We know, however, that in the continuum limit the pure ϕ^4 theory also becomes independent from the bare coupling λ, namely, the renormalized coupling is always zero. It is a very interesting possibility, that the λ-indepen-

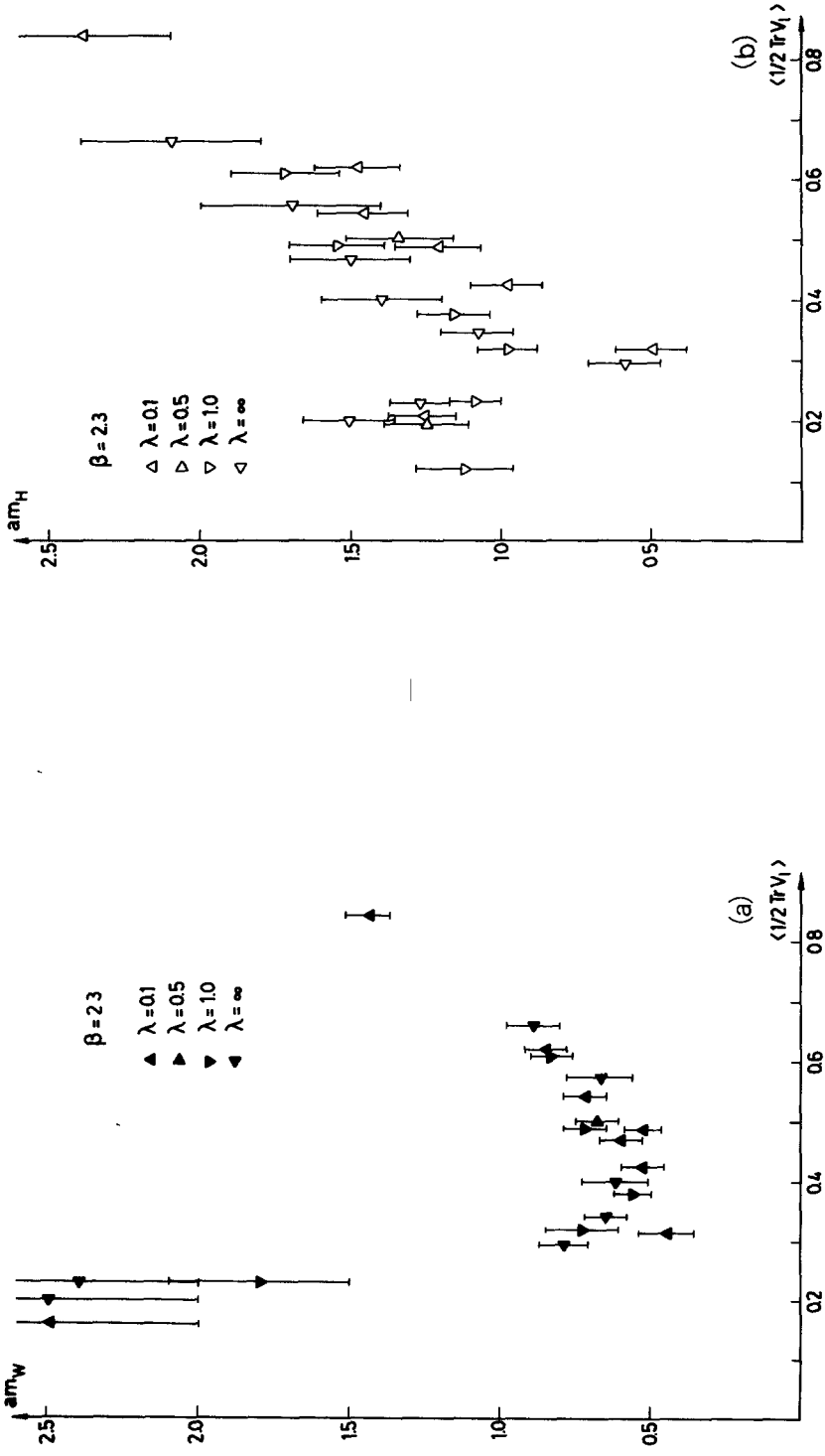

Fig. 4a. The W-boson mass in lattice units (am_W) as a function of the link expectation value $L = \langle \frac{1}{2} \operatorname{Tr} V_\ell \rangle$ for different λ-values at $\beta = 2.3$.

Fig. 4b. The same as fig. 4a, for the Higgs-boson mass (am_H)

dence of the continuum limit remains true after switching on the gauge coupling. This seems plausible in view of the asymptotic freedom of the gauge coupling, in particular if the continuum limit in the gauge-Higgs system is also at $\beta = \infty$.

The behaviour of the correlation lengths (or masses) near the phase transition is crucial also for the question of the order of the transition. The order of the phase transition is a statement concerning the behaviour of the system in the infinite volume limit, therefore the numerical investigation of the order has to include, obviously, a study of the lattice size dependence too. Some hints can, however, be obtained also on a fixed size lattice. Having this in mind, one can interpret the marked jump of the masses near $L = L_{cr} \simeq 0.26$ as a sign of the first-order nature of the confinement-Higgs phase transition for every positive λ. As it can be seen in figs. 4a and 4b, am_W jumps from values around $am_W \sim 0.5$ to $am_W \geqslant 2.0$. At the same time am_H jumps from $am_H \sim 0.5$ to $am_H \sim 1.2$, a value consistent with the 0^{++} glueball mass at the same β in SU(2) [19]. Another observation at the phase transition is that the average action per point s has a maximum near $\kappa = \kappa_{cr}$ (see fig. 5). This is what one can say on the basis of the present numerical data about the order of the phase transition. The important question of the order has to be investigated in detail in the future.

The position of the phase transition obtained from the correlations is substantially lower than the lines given in ref. [9] and shown also in fig. 1. The present best estimates for κ_{cr} are (always for $\beta = 2.3$):

$$\begin{aligned} \lambda = \infty: \quad & \kappa_{cr} = 0.386 \pm 0.005, \\ & \Delta\kappa \simeq 0.3; \\ \lambda = 1.0: \quad & \kappa_{cr} = 0.303 \pm 0.002, \\ & \Delta\kappa \simeq 0.09; \\ \lambda = 0.1: \quad & \kappa_{cr} = 0.192 \pm 0.001, \\ & \Delta\kappa \simeq 0.02. \end{aligned} \tag{2.19}$$

The $\Delta\kappa$ values give the approximate widths of the typical structure above $\kappa = \kappa_{cr}$ (for $\lambda \to 0$ $\Delta\kappa$ is expected to vanish like $\sqrt{\lambda}$).

Below the phase transition ($\kappa < \kappa_{cr}$) everything looks very much like in pure SU(2) gauge theory (further arguments in this direction will be given in the next section). In the Higgs phase ($\kappa > \kappa_{cr}$), far away from the phase transition, m_H is roughly twice as large as m_W. Near the critical line, however, m_H and m_W become nearly equal. Due to the somewhat large errors it is impossible at present to say whether there is a region for $\kappa > \kappa_{cr}$ also with $m_H < m_W$. For the moment, the numbers in the

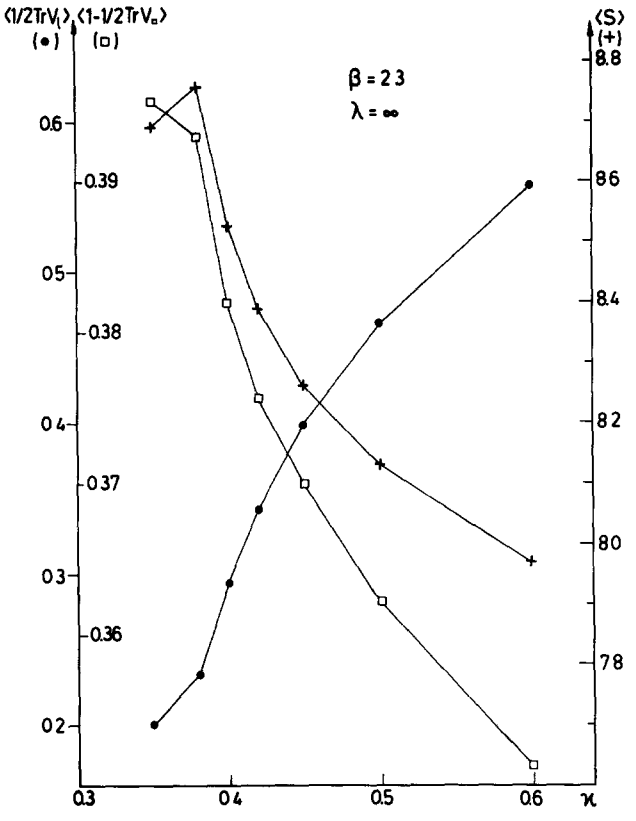

Fig 5 The κ-dependence of the average link $L = \langle \frac{1}{2} \operatorname{Tr} V_\ell \rangle$, average plaquette $P = \langle 1 - \frac{1}{2} \operatorname{Tr} V_P \rangle$ and average action per point s as defined in eq (2.18), for $\lambda = \infty$, $\beta = 2.3$. The lines are drawn just to guide the eye.

Higgs phase are consistent with $m_H \geq m_W$ (with error: $m_H \geq (1.0 \pm 0.3 m_W)$), but further Monte Carlo studies on larger lattices and with higher statistics can decide whether $m_H < m_W$ is possible in the Higgs phase or not. The lower bound $m_H \geq (1.0 \pm 0.3) m_W$ is probably also relevant (up to electromagnetic and fermionic corrections) to the real world with small gauge coupling, since m_H/m_W increases for decreasing gauge coupling strength (see the next section in connection with the discussion of the renormalization group trajectories).

Let us note that concerning the occurence of $m_H \simeq m_W$ the present conclusions differ from those of ref. [11]. The reason is the better statistics closer to the phase transition, which allows a more precise localization of the transition. Points with $m_H \simeq m_W$ were found in ref. [11] only near the endpoint of the phase transition line (near $\beta = 1.5$). Here we see that such points occur also at $\beta = 2.3$ (and probably also for every larger β), if one is going close enough (from above) to $\kappa = \kappa_{cr}$.

2.4 CORRELATIONS AT $\beta = \infty$

The $\beta \to \infty$ limit of the correlations can be numerically studied by a separate Monte Carlo simulation based on the action in eq. (2.12). This is equivalent to an O(4) σ-model in 4 dimensions, therefore the O(4) variables defined in (2.14) can also be used. For technical reasons, however, I took the SU(2) $\otimes$ SU(2) action (2.12) and used for the SU(2) site variables (α_x) the elements of the icosahedral subgroup.

Let us denote the inverse correlation length at $\beta = \infty$ measured by the Higgs field length variable ρ_x by am_h. For the inverse correlation length of the angular variables α_x let us introduce the notation am_g. In the continuum limit of the $\beta = \infty$ model m_h is the mass of the massive Higgs boson, whereas m_g is the mass of the 3 Goldstone bosons. We expect, namely, at some critical value $\kappa = \kappa_{cr}$ (which is a function of λ: $\kappa_{cr} = \kappa_{cr}(\lambda)$) spontaneous symmetry breaking. On the lattice this is manifested for $\kappa \geqslant \kappa_{cr}(\lambda)$ by a spontaneous alignment of the SU(2) variables in some arbitrary direction. The consequence of the spontaneous symmetry breaking SU(2) $\otimes$ SU(2) $\to$ SU(2) (or equivalently O(4) $\to$ O(3)) is the appearance of 3 massless Goldstone bosons ($am_g = 0$).

The Monte Carlo simulation at $\beta = \infty$ was carried out, similarly to the $\beta < \infty$ case, on an 8^4 lattice. In the Metropolis updating procedure the site variables α_x and ρ_x were updated simultaneously, with 6 hits per site (in a randomly chosen order of sites). Concerning the number of sweeps and the amount of statistics the same applies as for the finite β simulation (see above). The results obtained for am_g and am_h are shown in figs. 6a and 6b and in table 2. In the table the average link L, the average length ρ, the length dispersion σ_ρ and average action per site s are also included. These are defined, similarly to (2.18), as

$$
\begin{aligned}
L &= \left\langle \tfrac{1}{2} \mathrm{Tr}\left(\alpha^\dagger_{x+\mu}\alpha_x\right)\right\rangle , \\
\rho &= \langle \rho_x \rangle , \\
\sigma_\rho &= \sqrt{\langle \rho_x^2 \rangle - \langle \rho_x \rangle^2} , \\
s &= \langle \rho_x^2 - 3\log\rho_x + \lambda\left(\rho_x^2 - 1\right)^2 \rangle \\
&\quad + 8\kappa\left\langle 1 - \tfrac{1}{2}\rho_x\rho_{x+\mu}\mathrm{Tr}\left(\alpha^\dagger_{x+\mu}\alpha_x\right)\right\rangle .
\end{aligned}
\tag{2.20}
$$

As a function of the average link L, there is a similar approximate universality as for finite β (see fig. 7).

As it is shown by fig. 7, at the critical link expectation value $L = L_{cr} \approx 0.2$, spontaneous symmetry breaking takes place. Above this critical point the Goldstone boson mass (in lattice units) am_g is consistent with zero. At $L = L_{cr}$, on our 8^4 lattice, the Higgs mass am_h has a minimum value of $am_h = 0.4 \pm 0.1$. The critical κ

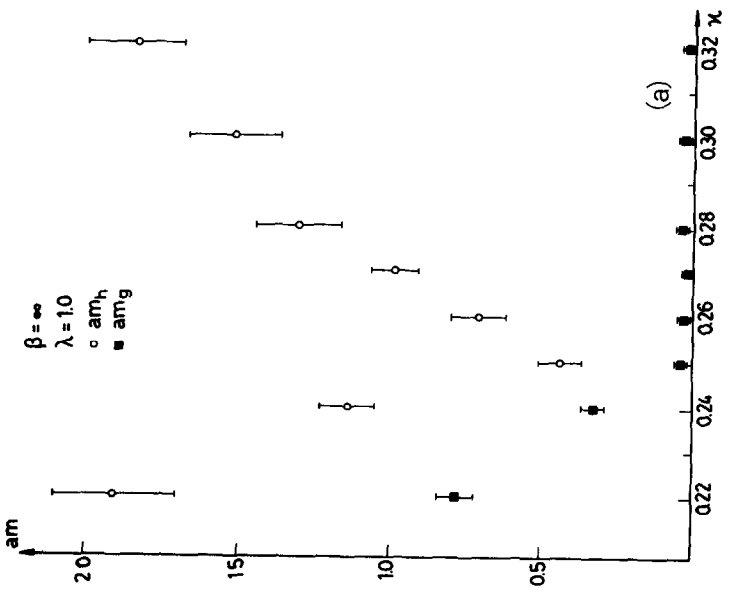

Fig. 6a. The inverse correlation lengths in the Goldstone boson (am_g) and Higgs boson (am_h) channel in lattice units in the σ-model at $\beta = \infty$ for $\lambda = 1.0$.

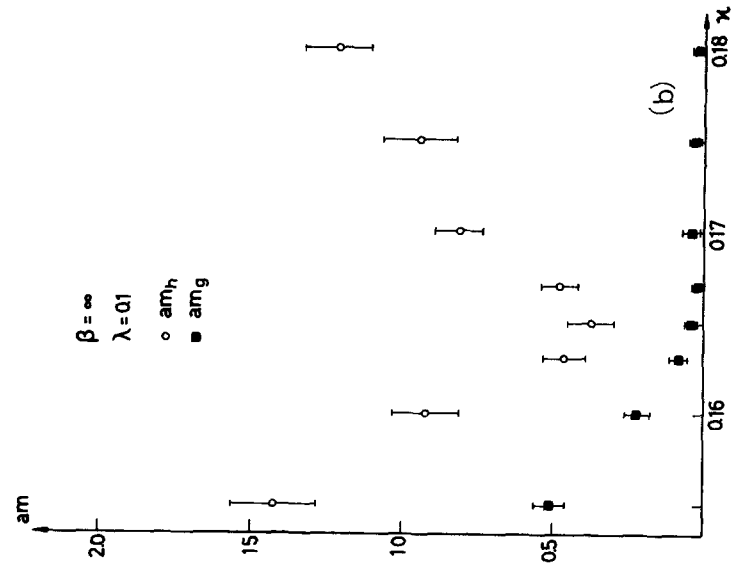

Fig. 6b. The same as fig. 6a, for $\lambda = 0.1$.

TABLE 2
The values of am_g and am_h for $\beta = \infty$

λ	κ	am_g	am_h	L	s	ρ	σ_ρ
1 0	0 22	0.78(6)	1.91(11)	0.1436(6)	2 876(7)	1 070	0 258
1 0	0 24	0 33(4)	1 14(9)	0 1717(3)	2 933(5)	1.081	0 259
1 0	0.25	0 04(2)	0.44(7)	0 2198(12)	2.856(6)	1 092	0 255
1 0	0 26	0.03(2)	0 71(9)	0.2954(14)	2.705(2)	1 124	0.256
1 0	0 27	0 02(2)	0 99(8)	0 3620(6)	2 551(8)	1 1490(4)	0 256
1 0	0 28	0 04(2)	1.31(14)	0 4180(9)	2 421(4)	1 173	0 249
1 0	0 3	0 03(2)	1.52(15)	0.5070(6)	2 169(5)	1 216	0 245
1 0	0.32	0 02(6)	1.85(16)	0.6361(4)	1.928(3)	1 256	0 241
0 1	0.155	0.51(5)	1 42(14)	0.1512(3)	2.262(2)	1 2901(8)	0 410
0 1	0 16	0 22(4)	0.92(11)	0 1664(4)	2 251(8)	1 3022(6)	0 413
0 1	0 163	0.08(3)	0 46(7)	0 1896(2)	2 207(3)	1 3191(2)	0.415
0 1	0 165	0.04(2)	0 37(8)	0 2269(5)	2 116(6)	1 346	0 417
0 1	0 167	0.02(2)	0 48(6)	0.2733(15)	2 014(9)	1 3793(7)	0.421
0 1	0 17	0 04(3)	0.81(8)	0 3401(12)	1 829(5)	1 430	0 426
0 1	0.175	0.03(2)	0 94(12)	0 4344(5)	1 570(3)	1 514	0 427
0 1	0 18	0.02(2)	1.21(11)	0.5079(14)	1 339(2)	1 5891(6)	0 427

The average quantities L, ρ, σ_ρ and s are defined in eq. (2 20) The errors in the last numerals are given in paranthesis If no error is given, the error estimate is $\leqslant 1$ in the last digit

at the two λ-values is, respectively:

$$\lambda = 1.0: \qquad \kappa_{cr} = 0.247 \pm 0.003\,,$$

$$\lambda = 0.1: \qquad \kappa_{cr} = 0.164 \pm 0.001\,. \tag{2.21}$$

The inverse correlation lengths around the critical point behave continuously (there is no jump like in figs. 4a–4b). This is consistent with the expected second-order phase transition. Above the critical point there are very long range correlations in the angular variables, extending practically over the whole lattice. In fact, the value of the angular correlation is typically only 5–10% smaller between the most distant ($d = 4$) time slices than for $d = 1$. In the limit $\kappa \to \kappa_{cr}$ the asymptotic behaviour of the correlations in the angular variables is expected to be power-like (it goes to zero like the inverse of the euclidean distance to the power $(2 + \eta)$, where η is some critical exponent [6]).

3. Static energies

3.1 WILSON LOOPS

The static energy $E(R)$ of an external SU(2) doublet charge pair is a characteristic property of the SU(2) gauge field system: in the case of confinement it increases

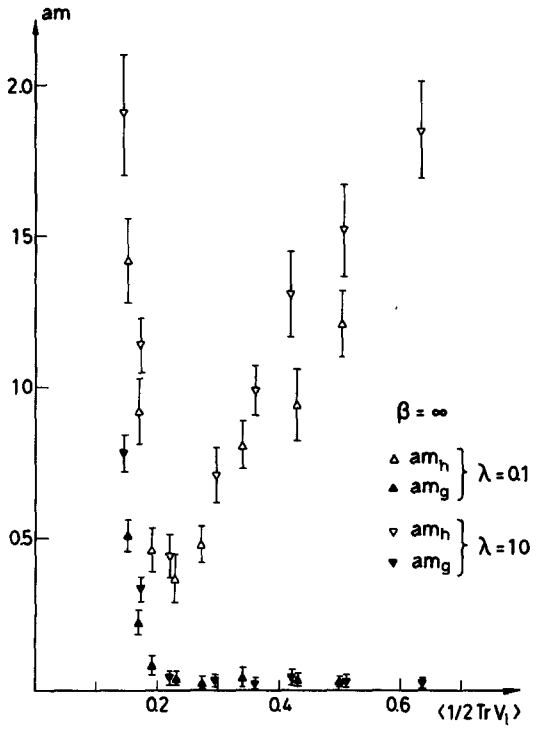

Fig. 7. The inverse correlation lengths in the σ-model at $\beta = \infty$ plotted as a function of the average link $L = \langle \frac{1}{2} \operatorname{Tr} V_\ell \rangle$ defined in eq (2.20).

linearly for large distances, whereas in a screening phase (like the Higgs phase) it goes asymptotically to a constant. As is well known, $E(R)$ can be determined from the expectation value of Wilson loops $W_{R,T} \equiv \frac{1}{2}\operatorname{Tr} U_{R,T}$ with time elongation T and euclidean distance R between the endpoints for fixed time:

$$aE(R) = -\lim_{T\to\infty} \frac{1}{T} \log W_{R,T}. \tag{3.1}$$

Some Monte Carlo measurements of the static energy $E(R)$ were performed on 8^4 lattice in ref. [11], where it was shown that rotation invariance of $E(R)$ is well satisfied if the largest correlation length is at least 1.

In this paper a more detailed study of the static energies will be presented. It was carried out on 12^4 lattice using the icosahedral subgroup for the SU(2) variables. The lattice actions (2.8) and (2.11) were used, and the Wilson loops were calculated from the gauge invariant links $V(x, \mu)$. This is equivalent, because of gauge invariance, to the use of the original link variables which appear in the definition of $W_{R,T}$. The values of planar Wilson loops with $1 \leqslant R$, $T \leqslant 5$ were determined (after 1000

TABLE 3a
The expectation values of Wilson loops $W_{R,T}$ in units of 10^{-5}

λ	β	κ	W_{11}	W_{12}	W_{13}	W_{14}	W_{15}
∞	2.0	0.55	57142(12)	35651(20)	22770(20)	14640(18)	09435(17)
∞	2.1	0.5	58983(9)	37855(14)	24833(15)	16384(14)	10827(12)
∞	2.1	0.6	60832(7)	40634(10)	27774(11)	19094(10)	13145(10)
∞	2 1	0.8	63142(7)	44145(10)	31524(11)	22647(11)	16287(11)
∞	2 3	0.3	60349(12)	38768(18)	25247(21)	16496(18)	10789(16)
∞	2.3	0.4	61805(10)	41123(16)	27848(19)	18946(18)	12906(17)
∞	2 3	0 45	63022(9)	43099(13)	30055(15)	21066(15)	14787(14)
∞	2 3	0.5	63759(6)	44257(9)	31339(10)	22306(10)	15900(10)
∞	2 3	0.6	64885(6)	46021(10)	33314(11)	24233(12)	17644(12)
∞	2 3	0.8	66529(6)	48599(8)	36215(9)	27106(10)	20316(10)
∞	2 4	0 4	64259(8)	44586(13)	31500(14)	22354(14)	15883(13)
∞	2.4	0 5	65631(6)	46819(10)	34052(11)	24883(11)	18206(11)
∞	2 4	0 6	66547(5)	48282(8)	35711(11)	26536(12)	19742(13)
∞	2 5	0 4	66155(8)	47246(12)	34341(14)	25073(16)	18328(16)
∞	2.5	0 45	66784(10)	48275(14)	35530(17)	26267(18)	19442(18)
1 0	2.3	0.32	62896(9)	42880(15)	29806(17)	20829(17)	14582(16)
1 0	2 3	0 35	64153(10)	44866(16)	32021(21)	22970(23)	16502(21)
1.0	2.3	0.4	65753(6)	47378(8)	34835(9)	25736(9)	19038(9)
0 1	2 3	0.195	62428(11)	42129(18)	28970(20)	20021(20)	13861(17)
0 1	2 3	0.205	64233(9)	44999(14)	32166(16)	23116(15)	16634(13)
0 1	2 3	0.22	66004(8)	47772(12)	35280(14)	26179(15)	19447(15)

TABLE 3b
The expectation values of Wilson loops $W_{R,T}$ in units of 10^{-5}

λ	β	κ	W_{22}	W_{23}	W_{24}	W_{25}	W_{55}
∞	2 0	0.55	16925(22)	08881(20)	04833(18)	02661(8)	00274(8)
∞	2.1	0.5	18783(18)	10212(15)	05722(12)	03238(10)	00385(7)
∞	2 1	0.6	22101(13)	13111(12)	07982(11)	04890(9)	00850(7)
∞	2.1	0.8	26323(12)	16984(12)	11168(12)	07382(10)	01794(8)
∞	2 3	0.3	18187(23)	09030(22)	04555(15)	02303(11)	00071(5)
∞	2.3	0.4	21263(23)	11814(23)	06715(18)	03858(15)	00351(7)
∞	2 3	0 45	23873(18)	14268(16)	08731(14)	05386(12)	00835(8)
∞	2.3	0.5	25380(13)	15696(13)	09928(11)	06324(11)	01189(10)
∞	2.3	0.6	27666(13)	17895(12)	11806(12)	07828(11)	01799(9)
∞	2.3	0.8	31013(11)	21161(11)	14677(10)	10225(9)	02958(9)
∞	2.4	0 4	25113(19)	15163(19)	09352(16)	05812(13)	00859(10)
∞	2.4	0.5	28145(13)	18149(14)	11934(13)	07901(12)	01722(9)
∞	2 4	0.6	30101(12)	20072(13)	13627(12)	09300(11)	02379(10)
∞	2.5	0 4	28083(17)	17822(18)	11532(18)	07522(16)	01388(11)
∞	2 5	0 45	29512(20)	19260(20)	12810(18)	08570(16)	01885(11)
1.0	2 3	0.32	23575(21)	13988(20)	08500(17)	05208(14)	00785(10)
1.0	2 3	0.35	26154(20)	16441(21)	10552(19)	06820(15)	01373(13)
1 0	2 3	0.4	29430(9)	19603(9)	13295(9)	09063(8)	02371(8)
0.1	2.3	0.195	22586(23)	13041(23)	07712(17)	04595(13)	00575(10)
0.1	2 3	0 205	26327(19)	16604(20)	10698(16)	06939(14)	01420(10)
0.1	2 3	0.22	29939(16)	20100(16)	13737(14)	09431(12)	02565(11)

TABLE 3c
The expectation values of Wilson loops $W_{R,T}$ in units of 10^{-5}

λ	β	κ	W_{33}	W_{34}	W_{35}	W_{44}	W_{45}
∞	2.0	0 55	04247(21)	02171(13)	01130(7)	01101(8)	00553(7)
∞	2 1	0 5	05059(14)	02658(9)	01430(7)	01356(9)	00720(6)
∞	2 1	0 6	07316(13)	04284(10)	02554(7)	02470(9)	01447(6)
∞	2.1	0.8	10561(12)	06790(10)	04401(8)	04333(10)	02795(8)
∞	2.3	0 3	03617(18)	01510(12)	00626(8)	00511(6)	00179(5)
∞	2.3	0.4	05798(18)	02999(14)	01579(10)	01459(11)	00731(8)
∞	2.3	0 45	07869(16)	04558(12)	02684(9)	02562(11)	01479(8)
∞	2.3	0.5	09092(13)	05503(10)	03379(9)	03255(10)	01981(8)
∞	2 3	0.6	11023(13)	07051(11)	04552(8)	04453(11)	02851(8)
∞	2.3	0 8	13960(12)	09478(11)	06479(9)	06376(10)	04342(8)
∞	2 4	0 4	08374(18)	04833(14)	02835(12)	02681(11)	01531(9)
∞	2 4	0 5	11045(12)	06989(14)	04472(9)	04339(10)	02739(8)
∞	2 4	0.6	12784(13)	08423(11)	05607(10)	05471(11)	03617(10)
∞	2 5	0 4	10492(18)	06434(16)	04008(12)	03822(14)	02331(10)
∞	2 5	0.45	11832(20)	07549(16)	04875(15)	04721(17)	03002(13)
1 0	2.3	0 32	07615(18)	04352(14)	02539(11)	02415(13)	01386(9)
1 0	2 3	0.35	09749(19)	06022(16)	03767(13)	03651(19)	02248(14)
1.0	2.3	0 4	12541(11)	08286(10)	05529(8)	05425(10)	03580(9)
0 1	2.3	0 195	06814(22)	03752(16)	02113(11)	01981(15)	01079(10)
0 1	2 3	0 205	09870(18)	06116(15)	03844(11)	03721(15)	02306(11)
0 1	2.3	0 22	12991(15)	08670(14)	05830(12)	05726(14)	03839(11)

equilibrating sweeps) in 2000–3000 sweeps for some selected points in the 3-dimensional parameter space (λ, β, κ). The results are collected in tables 3a–3c. This calculation took about 600 CPU hours on the Siemens 7.882 computer at the University of Hamburg.

Because of the limitation in the time elongation T, the best way to extract the static energy $E(R)$ is to fit the 5 points $(1 \leqslant T \leqslant 5)$ by the sum of two exponentials:

$$W_{R,T} = c_{1R}\exp(-\varepsilon_{1R}T) + c_{2R}\exp(-\varepsilon_{2R}T). \tag{3.2}$$

The industrious reader is invited to repeat the calculation on the basis of table 3. Here only the final results will shortly be summarized: the fit is good and the value of the smaller energy ε_{1R} is always stable with small error. Therefore, one can identify $aE(R)$ with ε_{1R}. The second energy ε_{2R} is also reasonably well determined, and its value is typically 3–6 times larger than ε_{1R} (typical values of ε_{2R} are in the range 1.6–2.3). This means that the field configuration around the external charge pair is sufficiently rigid and the static energy can be considered, to a good approximation, as a potential energy.

TABLE 4
Parameters of the potential in a Yukawa- (Y), Hulthén- (H) and string-like (S) fit defined by eq. (3 3)

λ	β	κ	fit	α	c	am	$a^2\sigma$
∞	2.0	0.55	S	0.305(15)	0.75(2)		0.003(3)
∞	2.1	0.5	Y,H	0.312(14)	0.66(2)	0 41(12)	
∞	2 1	0.6	Y,H	0.258(9)	0.538(4)	0.64(18)	
∞	2 1	0.8	Y,H	0 214(9)	0.441(2)	0 91(21)	
∞	2 3	0 3	S	0 192(22)	0.46(3)		0.160(10)
∞	2.3	0.4	S	0 274(8)	0 63(1)		0.032(3)
∞	2 3	0.45	S	0.250(5)	0.60(1)		0.002(2)
∞	2.3	0 5	Y,H	0.234(6)	0.52(1)	0.42(16)	
∞	2.3	0.6	Y,H	0 207(6)	0 453(2)	0.61(18)	
∞	2.3	0.8	Y,H	0.178(5)	0.387(1)	0.82(22)	
∞	2.4	0.4	S	0 241(5)	0 571(6)		0.0118(17)
∞	2 4	0.5	Y,H	0.206(5)	0.477(6)	0.33(15)	
∞	2.4	0.6	Y,H	0.191(5)	0 421(2)	0.60(19)	
∞	2.5	0.4	S	0.213(4)	0 519(5)		0 0067(14)
∞	2 5	0.45	Y,H	0.201(3)	0 48(1)	0.18(9)	
1.0	2.3	0.32	Y,H	0.264(3)	0.61(1)	0 14(7)	
1 0	2.3	0.35	Y,H	0.218(7)	0 50(1)	0.38(15)	
1 0	2.3	0.4	Y,H	0.187(5)	0.417(2)	0.69(21)	
0 1	2 3	0.195	S	0.277(5)	0.64(1)		0.0089(21)
0.1	2 3	0.205	Y,H	0.218(6)	0 49(1)	0.44(19)	
0 1	2.3	0.22	Y,H	0.190(6)	0 404(1)	0.81(25)	

The errors in paranthesis are the sums of statistical errors and estimated systematic errors.

The R-dependence of the potential for $1 \leqslant R \leqslant 5$ was compared to 3 simple forms:

$$\text{(Y)}: \quad -\frac{\alpha}{R}\exp(-amR) + c,$$

$$\text{(H)}: \quad -\frac{\alpha am}{\exp(amR) - 1} + c,$$

$$\text{(S)}: \quad -\frac{\alpha}{R} + a^2\sigma R + c. \tag{3.3}$$

Y stands for "Yukawa", H for "Hulthén" and S for a "string-like" potential. The best fit parameters are given in table 4, in those cases, when an acceptable fit could be obtained by the given form. The systematic errors of the fitting procedure were roughly estimated from the deviations in such cases, when different fits were possible.

As can be seen from table 4, the Yukawa- or Hulthén-form gives a good fit in the Higgs phase far enough from the phase transition surface. Therefore, the potential in these points is given, to a good approximation, by the massive W-boson exchange.

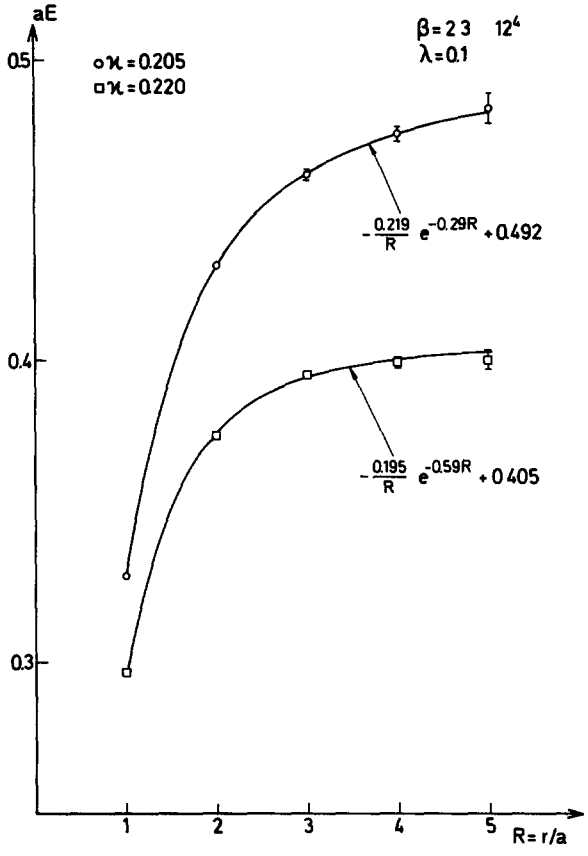

Fig 8. Typical examples of the static potential aE in such points, where the Yukawa form gives a good fit.

For typical examples see fig. 8. The fitted mass values am in table 4 are, within errors, consistent with the W-boson mass am_W determined from the correlations (see table 1). There is, however, some systematic difference between the Yukawa and Hulthén form: the former gives always smaller masses than the latter. Approaching the phase transition surface from above, the potential develops a quasi-linear, confinement-like behaviour for intermediate distances. The change between the pure Yukawa-like and more and more explicit string-like behaviour is continuous (for illustration see fig. 9). Near the phase transition the Yukawa fit gets gradually worse (see e.g. figs. 10a–b). It is expected, that in the Higgs phase at very large distances the potential finally tends always to a constant, but the turn-over might set in rather late. Eventually, it would be very interesting to know the exact behaviour at very large R. For instance, if the $R \to \infty$ form is given by const

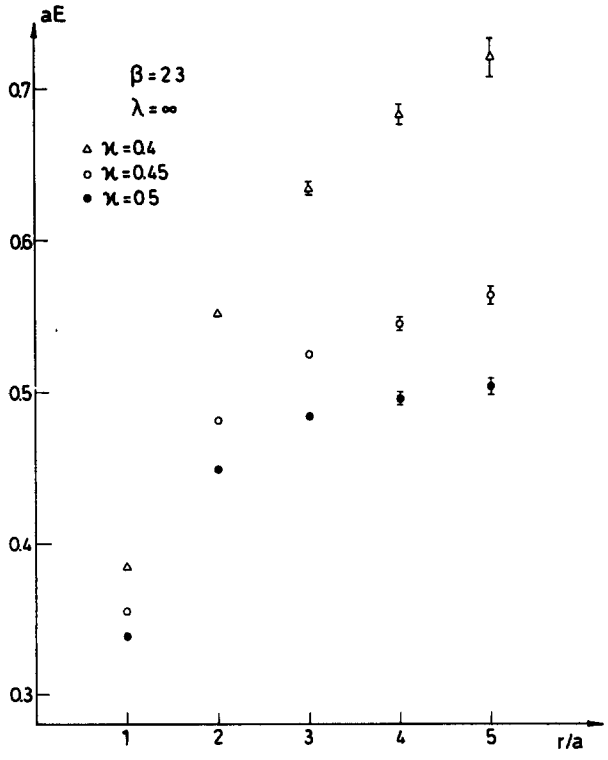

Fig. 9. The gradual change of the potential shape near the phase transition surface on the border of the Higgs-like region. The transition for $\lambda = \infty$, $\beta = 2.3$ is at $\kappa_{cr} = 0.386 \pm 0.005$

$-(\omega/R)\exp(-am_W R)$, then the value of ω could be quite different (e.g. much smaller) than the short-distance coupling α. Further Monte Carlo studies may give some hints in this direction, but this is presumably a rather difficult question for a numerical study. Below the phase transition surface the potential becomes rather similar to the pure gauge theory confinement potential. For instance, at ($\lambda = \infty$, $\beta = 2.3$, $\kappa = 0.3$) there is almost no difference compared to $\beta = 2.3$ in pure SU(2) gauge theory (see tables 3–4 and fig. 11).

Concerning the λ-dependence of the potential, if the average link L is used as a variable (like e.g. in figs 4a–b), then the same universal behaviour is observed as in the correlation lengths. For fixed λ the pattern of the short-distance behaviour of the potential can be characterized by the "renormalized gauge coupling" α obtained in the fits (3.3). This definition of the renormalized coupling is, of course, not very precise, because strictly speaking α is a function of R. But for a first qualitative understanding it is sufficient to consider the average defined by the fits. Taking the $\lambda = \infty$ values of α from table 4, a simple linear interpolation gives the curves of constant renormalized gauge coupling shown in fig. 12a.

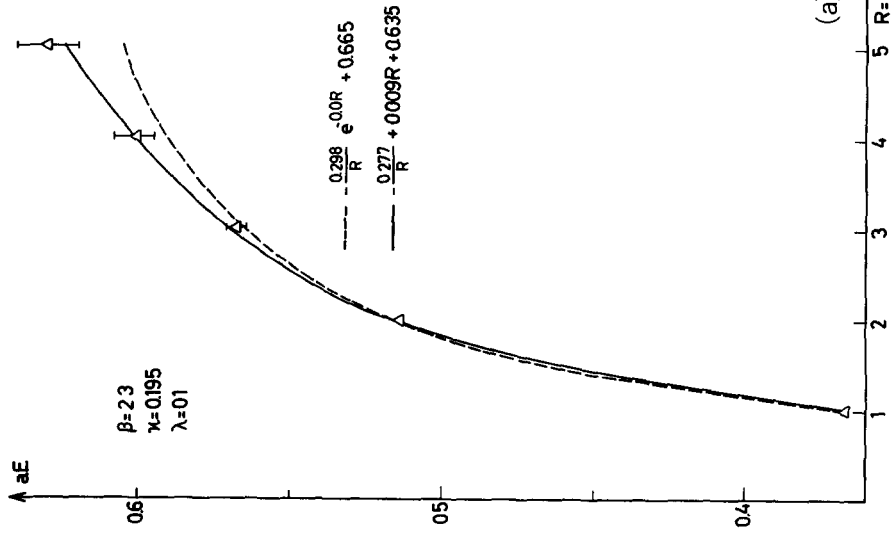

Fig. 10a. An example of the potential, where the Yukawa fit (dashed line) is much worse than the string-potential fit (full line). Note that the best Yukawa fit gives a mass $am \leqslant 0.0$, whereas the W-boson mass measured from the correlations is $am_W = 0.45 \pm 0.09$.

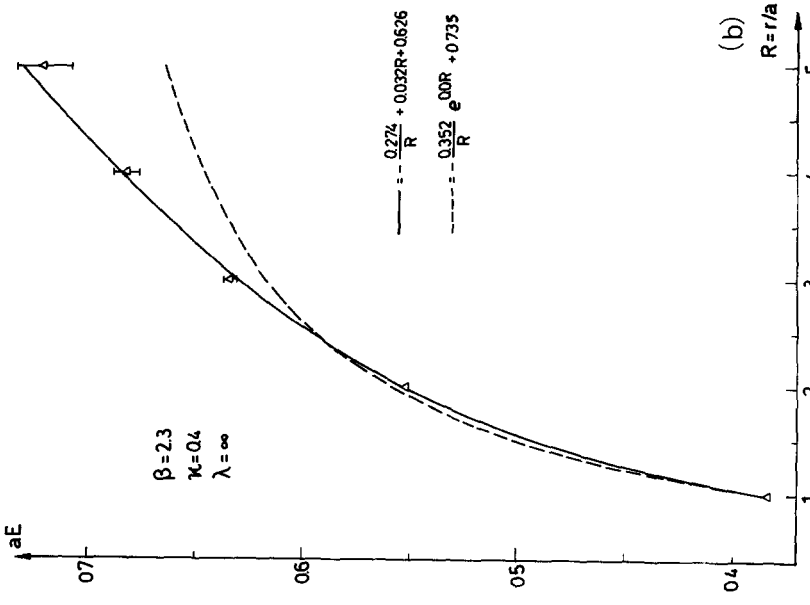

Fig. 10b Another example, where the Yukawa fit (dashed line) to the potential is very bad, but the string-potential fit (full line) is quite good. Note also here, that the best Yukawa fit requires $am = 0$, whereas the W-boson mass obtained from the correlations is $am_W = 0.79 \pm 0.08$.

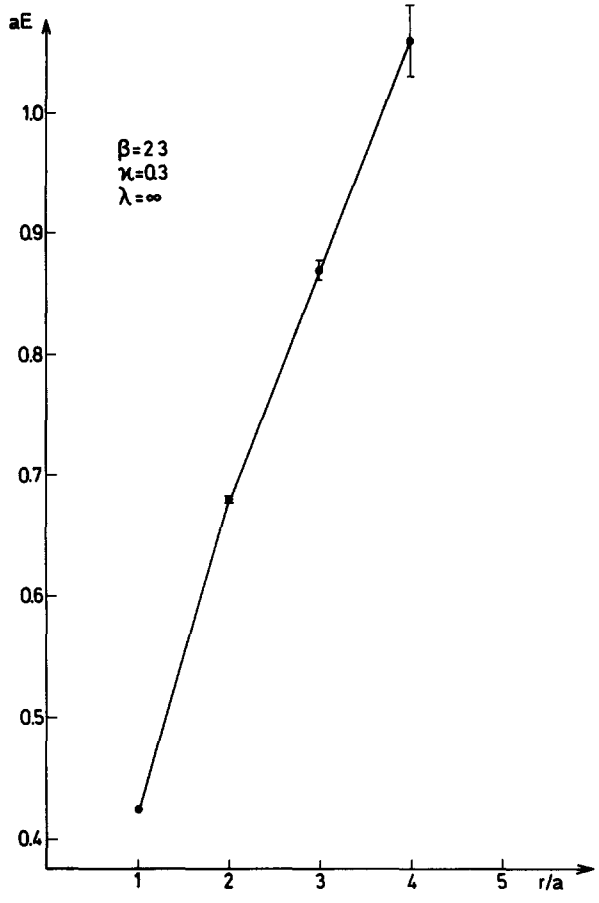

Fig. 11. The static potential in a point ($\lambda = \infty, \beta = 2.3, \kappa = 0.3$) below the phase transition surface ($\kappa < \kappa_{cr}$).

3.2 "CHIRAL" LOOPS

The potential energy deduced from Wilson loops refer to a pair of infinitely heavy particles, which are transforming as a vector-like (i.e. non-chiral) doublet under SU(2). In the SU(2) ⊗ U(1) electroweak theory the fermions (leptons and quarks) are in a chiral representation: left-handed fermions form doublets, but the right-handed ones are scalar. The chiral transformation property can influence the forces acting on a heavy particle. In order to have a feeling on this effect, let us consider heavy, chiral, naive fermions on the lattice. The fermion matrix in the bilinear fermion action can be written, in this case, like

$$Q = 1 - K\sum_{\mu}\left\{\frac{1-\gamma_5}{2}\gamma_\mu V(x,\mu) + \frac{1+\gamma_5}{2}\gamma_\mu\right\}. \tag{3.4}$$

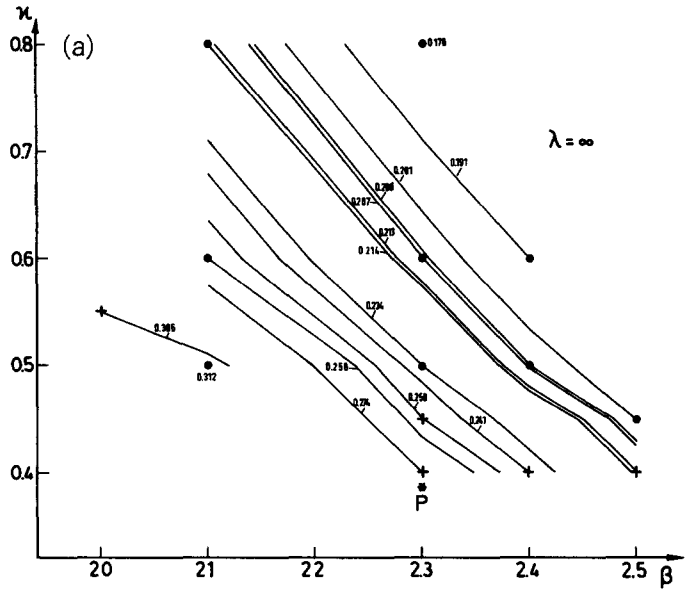

Fig. 12a. The curves of constant renormalized gauge coupling (α) for $\lambda = \infty$ in the (β, κ) plane. The lines were obtained from the potential fits given in table 4 by a linear interpolation. The point P gives the position of the phase transition at $\lambda = \infty$, $\beta = 2.3$.

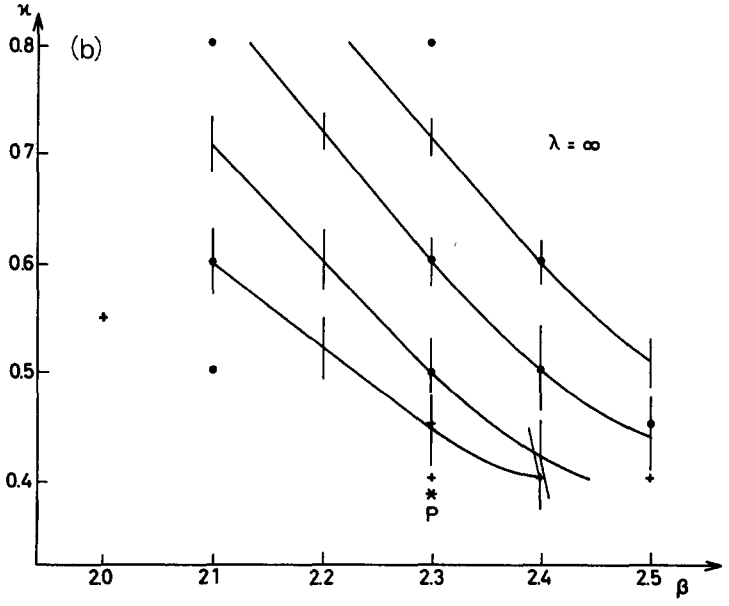

Fig. 12b. The RGT's in the studied region of the $\lambda = \infty$ plane given by the requirement of the rescaling of the force according to eq. (3.5). The vertical lines indicate the estimated errors.

Here $V(x, \mu)$ is the gauge invariant link variable introduced in the previous section and K is the hopping parameter inversely proportional to the mass. In the hopping parameter expansion, for very heavy fermions, only the shortest paths contribute. (For a review of the hopping parameter expansion see [20].) This gives the straight time-like sides of the Wilson loops for non-chiral fermions. In the case of (3.4) the dominant contribution for $K \to 0$ is again the straight line, but instead of a product of all link variables along the time-like sides, we have the product of every second (gauge-invariant) $V(x, \mu)$. For the space-like sides, representing the field between external charges, it is possible to take both a full product of all links or every second link (or even more complicated products of links). For the simplicity of comparison, let us take full products. In fig. 13 the potential extracted from such "chiral" loops is compared to the potential obtained in the same way from Wilson loops at $(\lambda = \infty, \beta = 2.3, \kappa = 0.5)$.As can be seen from the figure, the potential energy is reduced somewhat at larger distances by the chiral transformation property, but the overall qualitative behaviour remains the same.

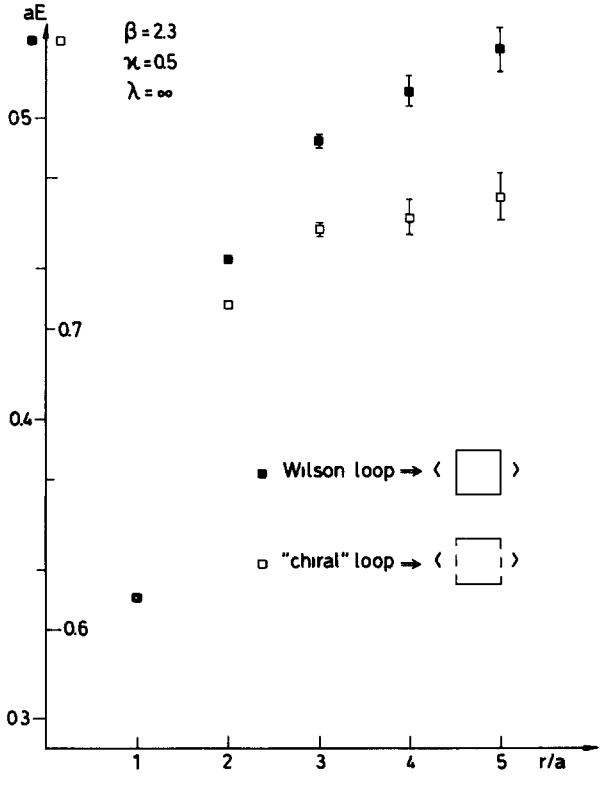

Fig 13 Comparison of the static potential extracted from the expectation values of Wilson loops and "chiral" loops. All the points shown were obtained from the ratio of loops with time elongation $T = 3$ and 5.

3 3 DIFERMION "ZOO"

The interesting consequence of the potential acting on a heavy fermion doublet pair is the possibility of bound states in the difermion channels due to the exchange of W-bosons. (Note that the SU(2) representations are real, therefore both fermions and anti-fermions feel the same potential.) Even a pure Yukawa potential of $-\alpha \exp(-mr)/r$ has bound states, if the coupling α is large enough and if the constituents are heavy enough. A short numerical investigation shows that the existence of at least one bound state in the non-relativistic Schrödinger equation is guaranteed for $\alpha M/m > 1$ (M is the reduced mass). The largest α-value in fig. 12 is around $\alpha \simeq \frac{1}{3}$, therefore $M/m_W > 3$ is enough. Of course, the quasi-confining potential shape near the phase transition line is even more favourable for bound states than the Yukawa-like potential.

3 4 RENORMALIZATION GROUP TRAJECTORIES

An important question in the lattice regularized SU(2) fundamental Higgs model is whether there exists a continuum limit defining a non-trivial (i.e. interacting) quantum field theory. The first complication compared to the pure gauge theory (where the existence of a non-trivial continuum limit is generally assumed, but up to now is not mathematically proven) is the presence of several independent couplings. The notion of renormalization group trajectories (RGT's) in such a case was discussed to the necessary degree of generality in the field theory and statistical physics literature (see, for instance, ref. [21]).

In order to see how these notions work in a specific (well-known) case with more than one coupling, let us consider QCD with a single (dynamical) quark mass. In this case there are two couplings: the gauge coupling g (or $\beta = 6g^{-2}$) and the dimensionless quark mass variable μ_q (for Wilson fermions one can define $\mu_q \equiv (2K_q)^{-1}$, where K_q is the hopping parameter). The renormalization group trajectories are conventionally parametrized by the renormalization group invariant quark mass M_q (more precisely, by the ratio M_q/Λ, where Λ is the usual RG Λ-parameter for the SU(3) gauge coupling). The expected shape of the scaling region and the RGT's $\mu_q = \mu_q(\beta, M_q)$ in the (β, μ_q) plane are shown in fig. 14. (For a more detailed discussion of QCD with dynamical quarks see ref. [20].) The curve $\mu_{cr}(\beta)$ is the line with zero quark mass $M_q = 0$ ($\mu_{cr}(\beta)^{1\,\mathrm{loop}}$ is its 1-loop perturbative approximation). The scaling region is, for $M_q \geqslant 0$, below the line (SQ). The critical point, where all the RGT's with constant M_q meet, is at $(\beta = \infty, \mu_q = 4)$. If only pure gluonic quantities (like glueball mass, string tension etc.) are considered, the scaling region is larger: it is for $M_q \geqslant 0$ the whole region to the right of the line (SG). For this reduced set of physical quantities there is only one relevant coupling (for instance β), and there exists an infinity of ("reduced") critical points along the line $\beta = \infty$, $4 < \mu_q \leqslant \infty$.

In the SU(2) fundamental Higgs model the study of correlations and static energies gives valuable information on the RGT's. Along the RGT's the mass ratio

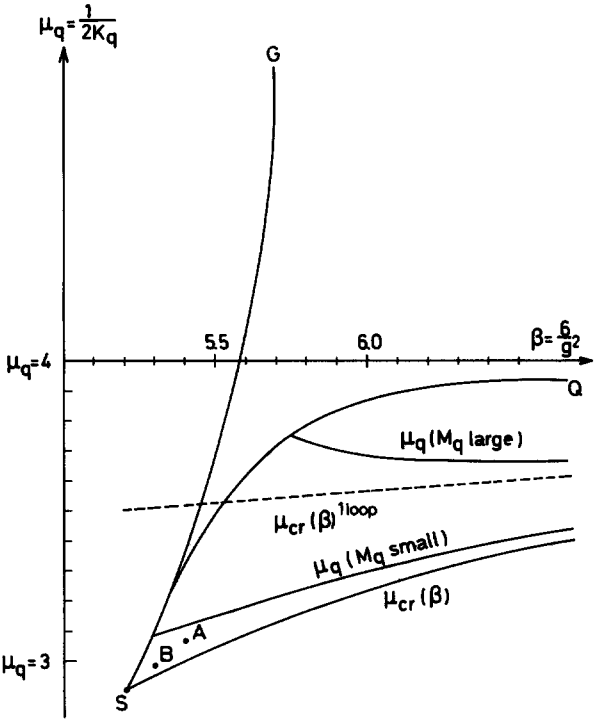

Fig. 14. The expected shape of the scaling region in the (β, μ_q) plane for QCD with $N_f = 3$ degenerate quark flavours. β is the SU(3) gauge coupling and μ_q is the quark mass parameter for Wilson fermions. The shape of the RGT's for small and large RG invariant quark mass M_q is shown. The meaning of the other curves is explained in the text. A spectrum calculation with dynamical quarks was performed in ref. [24] for ($\beta = 5.4, \mu_q = 3.0675$) and ($\beta = 5.3, \mu_q = 2.9762$). These points are denoted, respectively, by A and B. The RGT's with constant M_q and the critical line $\mu_{cr}(\beta)$ tend for $\beta \to \infty$ to $\mu_q = 4$.

m_H/m_W has to be constant, and the force $a^2 \mathrm{d}E(r/a)/\mathrm{d}r \equiv F(R)$ acting on the external doublet pair at physical distance $r = aR$, can be scaled between two points with scale ratio $\xi_{12} = a_2/a_1$ as

$$F_1(R) = \xi_{12}^{-2} F_2\left(\frac{R}{\xi_{12}}\right). \tag{3.5}$$

If the static energy is determined for N different distances, the force represents $(N-1)$ different physical quantities. Since the static energy can be obtained with good precision, eq. (3.5) gives an accurate constraint on the RGT's. In fact, the scaling properties of the potential can be used in pure SU(2) gauge theory for the precise determination of the scale ratio ξ_{12} [22]. In the Higgs phase the shape of the potential changes gradually from Yukawa-type to a quasi-confinement form

near the phase transition surface in the (λ, β, κ) space. Therefore, the RGT's can be pinned down by the requirements of a constant shape.

Starting from the Wilson loop values measured in discrete points of the parameter space, first one has to interpolate them in some region. Because of the universality in λ, I considered only the $\lambda = \infty$ plane and took, for simplicity, a linear interpolation between the measured points. (The points are shown, for instance, in fig. 12a.) The force $F(R)$ can be defined in an arbitrary point by fitting the potential with one of the forms in eq. (3.3), and then by the requirement of rescaling according to eq. (3.5) it is possible to decide whether a point pair is on the same RGT or not. Choosing different combinations of point pairs and comparing the scale factors, it is also possible to check the systematic errors of this procedure. A source of systematic errors is the interpolation of the Wilson loop expectation values. This can, in principle, be easily decreased by using a higher order interpolation and/or by measuring on a denser set of points. Another, potentially more dangerous, source of errors is the use of the fits (3.3) for the definition of the force. I checked this by defining the force also from a quadratic interpolation between neighbouring potential points. The results turned out to be consistent with the results of the fitting procedure. In the vicinity of the phase transition the interpolation procedure was even more stable. The resulting shape of RGT's is shown in fig. 12b. Although the errors on the curves are not small, some qualitative consequences can immediately be drawn. For instance, the picture is completely inconsistent with a critical point at the end of the phase transition line near $\beta \simeq 1.5$ (see fig. 1). All the numerical information (including the masses am_{H} and am_{W}) is consistent with a critical point at the $\beta = \infty$ end of the phase transition line, which coincides with the critical point of the σ-model for the given, fixed λ-value.

As it was discussed in detail previously, the masses and static energies are approximately universal functions of the link expectation value L (see figs. 4a–4b and 7). This means that there exists a mapping between any two planes $\lambda = \lambda_1$ and $\lambda = \lambda_2$ such that the physical quantities do not change. Assuming that the small deviations from universality either are due to lattice artifacts (i.e. disappear in the continuum limit) or can be transformed away by optimizing the mapping, it follows that the continuum limit is independent from λ. In other words, the number of independent parameters in the continuum theory is smaller than in the regularized theory: the same parameter reduction occurs in the gauge-Higgs system as in the pure ϕ^4 theory.

Below the phase transition line in the (β, κ) plane there might also be RGT's corresponding to a confining theory with scalar matter fields and zero vacuum expectation values (as advocated in ref. [7]). In the present data we see no evidence for this, because everything measured below the phase transition line looks very similar to pure gauge theory. Nevertheless, in future Monte Carlo studies one should go very close to the phase transition line from below, perhaps also at larger β-values, in order to have better constraints. Of course, a direct Monte Carlo renormalization

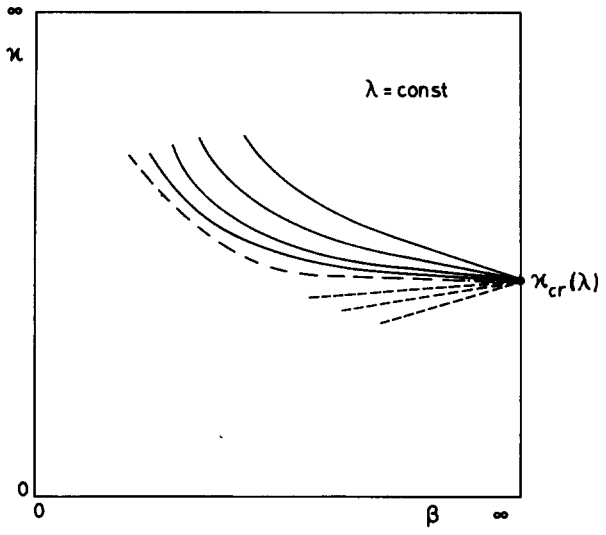

Fig. 15. The schematic behaviour of the renormalization group trajectories in the (β, κ) plane for any $\lambda = \text{const} > 0$ The phase transition line is dashed-dotted. The full lines are the RGT's in the Higgs-like phase The dashed lines could be RGT's in the confinement-like phase, which tend to the critical point from below the phase transition line.

group [23] study of the RGT's, both in the Higgs- and confinement-like phases, would be desirable. The expected picture of the RGT's in the $\lambda = \text{const}$, planes is schematically shown in fig. 15.

4. Conclusion

The numerical Monte Carlo study of correlations and static energies in the SU(2) gauge theory with a Higgs-scalar doublet is rather useful for the understanding of continuum physics behind the lattice-regularized theory. In this paper numerical evidence was found for the (at least approximate) irrelevance of the Higgs self-coupling λ. The renormalization group properties in the two relevant couplings (β, κ) are qualitatively similar to the situation in QCD with a single (dynamical) quark mass. It is expected, that for any fixed positive λ there is a single critical point at $\beta = \infty$, $\kappa = \kappa_{cr}(\lambda)$ (where $\kappa_{cr}(\lambda)$ is the critical point in the σ-model at $\beta = \infty$).

The marked jump found in both the W-boson and Higgs boson mass at the confinement-Higgs phase transition can be a hint for the first-order nature of the transition for any λ, but for a decision between second order and weakly first order further detailed studies are necessary. Below the phase transition surface, there might be RGT's which define a confining continuum theory with scalar matter fields. The present data give no evidence for this, because every measured quantity looks, below the transition surface, very similar to pure SU(2) gauge theory.

In the Higgs phase there is a lower bound for the ratio of the Higgs mass to W-mass:

$$\frac{m_{\mathrm{H}}}{m_{\mathrm{W}}} \geqslant 1.0 \pm 0.3 . \tag{4.1}$$

This relation was obtained in the region with strong gauge coupling, but presumably it holds also for weak gauge coupling (up to electromagnetic and fermionic corrections), because $m_{\mathrm{H}}/m_{\mathrm{W}}$ increases with decreasing (renormalized) gauge coupling. If there are, indeed, only two relevant couplings, then the physical value of $m_{\mathrm{H}}/m_{\mathrm{W}}$ is uniquely determined by the renormalized gauge coupling. The direct Monte Carlo evaluation of $m_{\mathrm{H}}/m_{\mathrm{W}}$ for the phenomenologically interesting weak gauge coupling seems difficult. A possible way is to go into the σ-model at $\beta = \infty$, and calculate m_{W} from the mass parameter f_{g} characterizing the spontaneous symmetry breaking $\mathrm{SU}(2) \otimes \mathrm{SU}(2) \to \mathrm{SU}(2)$. (In the context of QCD f_{g} is usually denoted by f_{π}.) A possible way to extract f_{g} by a Monte Carlo simulation in the σ-model was proposed recently by Dashen and Neuberger [15]. The numerical calculation seems not very easy, but it is certainly worth a try.

It is a pleasure to acknowledge discussions with Peter Hasenfratz, Martin Lüscher and Roberto Peccei. Their remarks contributed in an essential way to the final form of this paper. I am indebted to Christian Lang for a correspondence about his Monte Carlo data. I wish to thank the Computer Centre of the University of Hamburg for the generous support of the computations in this paper.

References

[1] A. Peterman, Phys. Reports 53C (1979) 157
[2] UA1 Collaboration, Phys. Lett 122B (1983) 103; 126B (1983) 398;
UA2 Collaboration, Phys Lett. 122B (1983) 476; 129B (1983) 130
[3] P W. Higgs, Phys Lett. 12 (1964) 132; Phys. Rev. Lett 13 (1964) 508; Phys. Rev 145 (1966) 1156;
F. Englert and R. Brout, Phys. Rev. Lett. 13 (1964) 321;
G.S. Guralnik, C R. Hagen and T.W. Kibble, Phys. Rev. Lett 13 (1964) 585;
T W B. Kibble, Phys Rev 155 (1967) 1554
[4] Lattice gauge theories and Monte Carlo simulations, ed. C Rebbi (World Scientific, 1983)
[5] P.V.D. Swift, Phys. Lett 145B (1984) 256
[6] K.G Wilson, Phys. Rev. B4 (1971) 3184;
K G. Wilson and J. Kogut, Phys. Reports 12C (1974) 75;
R. Schrader, Phys. Rev. B14 (1976) 172;
B. Freedman, P. Smolensky and D. Weingarten, Phys. Lett. 113B (1982) 481;
M. Aizenmann, Phys Rev Lett. 47 (1981) 1; Commun. Math. Phys. 86 (1982) 1;
J. Fröhlich, Nucl. Phys B200 [FS4] (1982) 281;
C. Aragão de Carvalho, C S. Caracciolo and J. Fröhlich, Nucl. Phys B215 [FS7] (1983) 209;
J Fröhlich, *in* Progress in gauge field theory, Cargese lecture 1983, ed. G. 't Hooft et al. (Plenum, 1984)
[7] L.F. Abbott and E. Fahri, Phys Lett. 101B (1981) 69
[8] C.B. Lang, C. Rebbi and M. Virasoro, Phys. Lett 104B (1981) 294;
M. Creutz, L. Jacobs and C. Rebbi, Phys. Reports 95C (1983) 201

[9] H. Kühnelt, C.B. Lang and G. Vones, Nucl. Phys. B230 [FS10] (1984) 31
[10] M Tomiya and T. Hattori, Phys. Lett. 140B (1984) 370
[11] I. Montvay, Phys. Lett. 150B (1985) 441
[12] E. Fradkin and S. Shenker, Phys. Rev. D19 (1979) 3682;
G. 't Hooft, Cargese Summer Institute lecture, 1979;
T. Banks and E. Rabinovici, Nucl. Phys. B160 (1979) 349;
S. Dimopoulos, S. Raby and L. Susskind, Nucl. Phys B173 (1980) 208
[13] M. Veltman, Acta. Phys. Pol B8 (1977) 475;
B W. Lee, C. Quigg and H.B. Thacker, Phys. Rev. D16 (1977) 1519;
T. Appelquist and C. Bernard, Phys. Rev. D22 (1980) 200;
A. Longhitano, Phys. Rev. D22 (1980) 1166
[14] M.B. Einhorn, Nucl. Phys. B246 (1984) 75
[15] R. Dashen and H. Neuberger, Phys. Rev. Lett. 50 (1983) 1897
[16] M. Gell-Mann and M. Lévy, Nuovo Cim. 16 (1960) 705
[17] W.A. Bardeen and M. Moshe, Phys. Rev. D28 (1983) 1372
[18] B. Berg, S. Meyer and I. Montvay, Nucl. Phys B235 [FS11] (1984) 149
[19] H. Meyer-Ortmanns and I. Montvay, Phys. Lett. 145B (1984) 251
[20] I. Montvay, DESY preprint 85-072 (1985)
[21] K.G. Wilson and J Kogut, Phys. Reports 12C (1974) 75;
E. Brézin, J.C. Le Guillou and J. Zinn-Justin, *in* Phase transitions and critical phenomena, ed. C. Domb, M.S Green (Academic Press, London, 1976) vol. 6, p. 125
[22] F Gutbrod and I. Montvay, Phys. Lett. 136B (1984) 411
[23] S.K Ma, Phys. Rev. Lett. 37 (1976) 461;
R.H. Swendsen, Phys. Rev. Lett. 42 (1979) 859;
K.G. Wilson, *in* Recent developments of gauge theories, ed. G. 't Hooft et al. (Plenum, 1980);
A. Hasenfratz, P. Hasenfratz, U. Heller and F. Karsch, Phys. Lett. 140B (1984) 76
[24] W. Langguth and I. Montvay, Phys. Lett. 145B (1984) 261